

Effect of MC Type Carbides on Age Hardness and Thermal Expansion of Fe–36 wt%Ni–0.2 wt%C Alloy

K. Nakama · K. Sugita · Y. Shirai

Received: 23 August 2013/Revised: 11 October 2013/Accepted: 11 October 2013/Published online: 24 October 2013
© Springer Science+Business Media New York and ASM International 2013

Abstract Fe–36 wt%Ni alloy, also called “Invar alloy”, is known for its low-thermal expansion. Since it has only mediocre strength and accordingly its application is limited, effects of addition of several carbide-forming elements, Ti, V, Zr, Nb, and Ta, on age hardness and thermal expansion of Fe–36 wt%Ni–0.2 wt%C alloy were studied for the purpose of developing a high-strength and low-thermal expansion alloy. All the alloys except Zr-added sample showed maximum hardness when aged at 650 °C. Among these additives, V had the largest age-hardenability with vanadium carbides precipitated abundantly and finely. In addition, vanadium carbides were formed with their crystallographic axes parallel to the matrix, causing about 15% of misfit strain. In the viewpoint of strengthening by carbide precipitation, large solubility in the matrix and structure and lattice constant similar to the austenitic matrix are important, and V is a preferred additive to Fe–36 wt%Ni–0.2 wt%C alloy. On the other hand, the V-added alloy in solution-treated condition showed the largest thermal expansion coefficient near room temperature. This was because it composed of larger amount of C and V in solid solution state but it is expected that its thermal expansion will decrease when these elements are eliminated from the matrix by appropriate aging.

Keywords Iron · Nickel · Invar · Aging · Carbide · Hardness · Thermal expansion

Introduction

Fe–36 wt%Ni alloy is well-known as Invar alloy for its low-thermal expansion (Invar effect) near ambient temperature [1]. The Invar effect originates from the fact that the normal lattice expansion with temperature elevation is balanced out by the contraction due to the negative volume magnetostriction. Thermal expansion coefficient (TEC) of Fe–36wt %Ni alloy is about one tenth of that of steel and the alloy is widely used for precision parts where variation in length with temperature is unfavorable [2]. However, Fe–36 wt%Ni alloy has relatively low strength for structural members and its application has been limited. There, in fact, are some strengthened Invar alloys designed for core cables of high-voltage power transmission lines [3–5]. Used for core cables, the strengthened Invar alloys prevent the power lines from sagging because thermal expansion caused by Joule heat is minimized. These alloys are strengthened by cold-working and following aging heat treatment. During aging, precipitation hardening by alloy carbides occurs and, as a consequence of elimination of C and other alloy elements from the matrix, thermal expansion tends to become smaller [6]. For these reasons, favorable alloy elements as strengthening additives should have strong affinity to C and effective age-hardenability. Among carbide-forming elements, those which form NaCl type carbides are of great interest. This is because NaCl structure is similar to the Fe–36 wt%Ni austenitic matrix and, depending on element selection, lattice constant of the carbide could be close to that of the matrix, which would be expected to enhance the magnitude of precipitation

K. Nakama (✉)
Research & Development Center, Sanyo Special Steel Co., Ltd.,
3007, Nakashima, Shikama-ku, Himeji-shi 672-8677, Japan
e-mail: knakama@himeji.sanyo-steel.co.jp

K. Sugita · Y. Shirai
Department of Materials Science and Engineering,
Faculty of Engineering, Kyoto University,
Kyoto 606-8501, Japan

strengthening by misfit strain effect. In this context, difference of NaCl type carbide-forming elements, Ti, V, Zr, Nb, and Ta, are focused and effects of these additives to Fe–36 wt%Ni–0.2 wt%C alloy on precipitates, age hardness and thermal expansion are studied.

Experimental

One kilogram ingots of Fe–36 wt%Ni–0.2 wt%C–X alloys, hereafter called Invar-X, where X was Ti, V, Zr, Nb, or Ta, were prepared by a vacuum induction furnace. Chemical compositions of these alloys are shown in Table 1. Amounts of these elements were adjusted so that atomic ratios of the carbide-forming elements to C were nearly unity. The ingots were forged at 1150 °C to round bars with a size of 15 mm in diameter. Subsequently, solution heat treatment was carried out at 1200 °C for 30 min followed by water quenching. In order to obtain work- and age-hardenability, round-bar type specimens with a size of 8 mm in diameter and 12 mm in length were compressed in the longitudinal direction by 20–60 % at a strain rate of 0.1/s at room temperature and those specimens which had been compressed by 40% were heat-treated in the temperature range 550–750 °C for 2 h, followed by hardness measurement by a Vickers hardness testing machine. Scanning electron microscope (SEM) and transmission electron microscope (TEM) observations were performed for some of the aged specimens to see the precipitated carbide morphology. Samples for SEM observation were prepared by mirror-polishing and flat-milling with Ar atoms. Thin foil specimens manufactured by jet-polishing and extracted replica specimens in an acetylacetone solution were used for TEM observation. For thermal expansion measurement, the round-bar type specimens with a size of 3 mm in diameter and 10 mm in length were used. TECs were calculated from dilation curves by a dilatometer at a heating rate of 3 K/min from room temperature to 300 °C.

Results and Discussion

Compressed and Aged Hardness

Figure 1(a) shows the change in hardness with alloy compositions and compression ratio. Hardness of a similarly conditioned Fe–36 wt%Ni alloy is also shown in the figure. In solution-treated condition, hardness of Invar-V was the highest. When compressed, Invar-V underwent the largest work-hardening, followed by Invar-Ti and other alloys. After aging heat treatments, all the alloys except Invar-Zr showed more or less age hardening as shown in

Table 1 Chemical composition of the studied alloys (wt%)

| Alloy | Fe | C | Si | Mn | Ni | Co | Others | X/C ^a |
|----------|------|-------|------|------|-------|-------|----------|------------------|
| Invar-Ti | Bal. | 0.204 | 0.21 | 0.20 | 35.53 | <0.01 | Ti: 0.83 | 1.02 |
| Invar-V | Bal. | 0.203 | 0.22 | 0.19 | 35.80 | <0.01 | V: 0.80 | 0.93 |
| Invar-Zr | Bal. | 0.207 | 0.21 | 0.19 | 36.10 | <0.01 | Zr: 1.07 | 0.68 |
| Invar-Nb | Bal. | 0.189 | 0.21 | 0.20 | 35.72 | <0.01 | Nb: 1.34 | 0.92 |
| Invar-Ta | Bal. | 0.180 | 0.23 | 0.19 | 36.26 | <0.01 | Ta: 2.96 | 1.09 |

^a X/C: atomic ratio of X–C, X = Ti, V, Zr, Nb, or Ta

Fig. 1(b). Invar-V had the largest age-hardenability with the peak hardness 310 HV after aging at 650 °C. Invar-Ti, Invar-Nb, and Invar-Ta also showed the maximum hardness when aged at 650 °C, though the increases in hardness by aging were smaller than that in Invar-V. Invar-Zr reduced its hardness monotonously with rise in aging temperature.

Carbide Morphology

Since alloy compositions other than element X (X = Ti, V, Zr, Nb, or Ta) are almost the same for the studied sample, the difference in age hardness should be attributed to the contribution by these elements. SEM images of the carbides of Invar-X's in 40% compressed and 650 °C aged condition are shown in Fig. 2. Brighter particles in the figure are carbides that comprise mainly of carbide-forming element X. Because a resolution of SEM is limited, infinitesimal carbides were not captured. Invar-Ti, Zr, Nb, and Ta contained many relatively large carbides the sizes of which reached the order of from 100 nm to 1 μm. Only Invar-V contained few large carbides but had fine precipitates smaller than 100 nm.

Solubility products in austenite of the carbides employed in this study is reported as shown in Table 2 [7]. Even at as high as 1200 °C, which is a temperature adopted for solution treatment in this study, considerable large amount of carbides except VC remain undissolved in the matrix. VC has much larger solubility in austenitic phase than any other elements. This means that the amount of precipitated carbide after aging is large for Invar-V since the solubility of carbides are very small at 650 °C. In addition, VC has the nearest lattice constant to the austenite matrix. Figure 3 shows results of electron microscope observation for Invar-V. In Fig. 3(a), an electron diffraction image taken from a selected area demonstrated two overlapped patterns one of which was about 15% smaller than the other. Judging from the spacing and angles between the spots, the larger pattern is the diffracted pattern from the austenite matrix with the zone axis [001]. The smaller one, on the other hand, is similar structure to the matrix and has the larger spacing in real space. The calculated spacing between {220} planes of the smaller pattern are

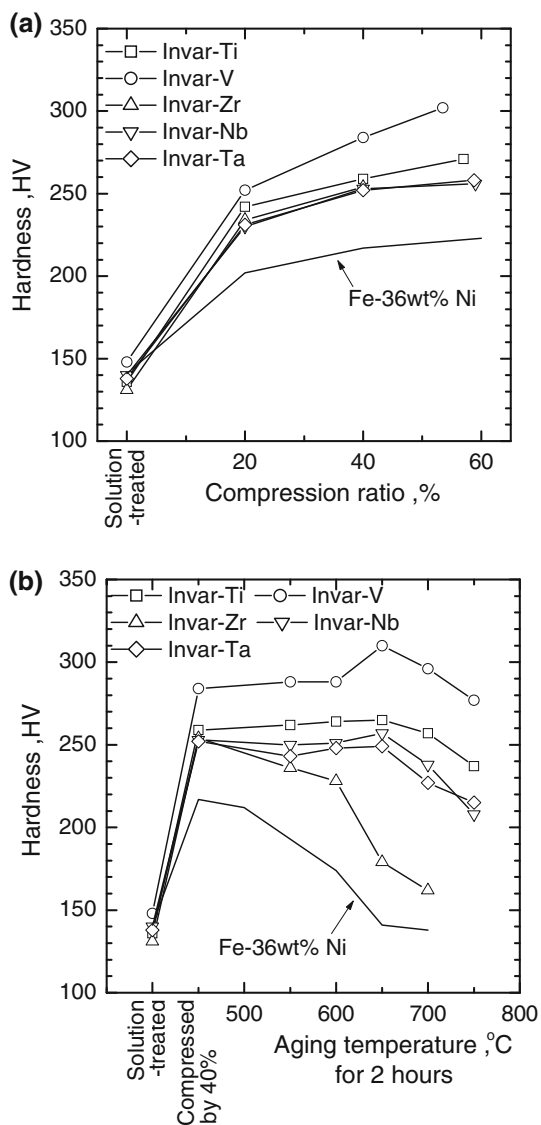


Fig. 1 Hardness of Invar-X after compression and aging heat treatment: (a) effect of addition of Ti, V, Zr, Nb, and Ta on work-hardening ability, (b) effect of addition of Ti, V, Zr, Nb, and Ta on age hardness

0.141 nm, which is close to {220} spacing of vanadium carbide, 0.146 nm (VC_{0.75}) and 0.148 nm (VC). The fact that {220} and {−200} planes of the FCC matrix and the vanadium carbide are parallel each other means that the carbides precipitated coherently with significant misfit strain. Figure 3(b) is a dark-field image captured by collecting the diffracted spot in a white circle in Fig. 3(a). Bright particles in Fig. 3(b) correspond to the locations where the smaller diffraction pattern came from. Combining the above results, these particles are vanadium carbides precipitated finely with their axis parallel to the matrix, although the existence of the carbides is unable to see in the bright field image in Fig. 3(c). Figure 3(d) shows an image of an extracted replica. Particles with a size of 5 nm are visible and they are recognized as

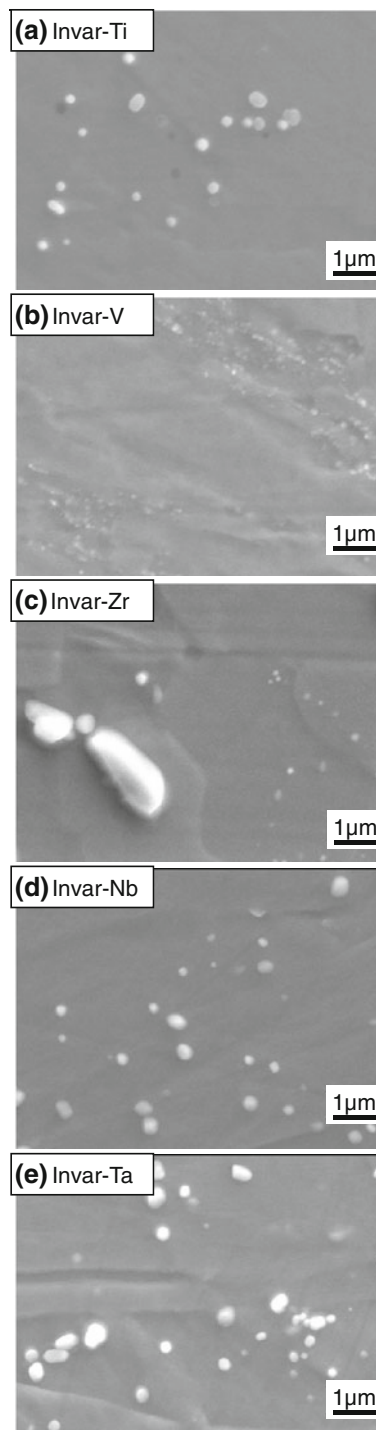


Fig. 2 Carbide morphology of Invar-X in 40% compressed and 650 °C-aged condition

vanadium carbides by a diffraction pattern measurement and an EDS analysis.

According to the particle precipitation-strengthening model, the strengthening with misfit strain is known to be:

$$\tau^\infty G\epsilon^{3/2}(r \cdot f)^{1/2} \tag{1}$$

Table 2 Solubility products of XC type carbides in austenitic region of steel [7]

| Carbide | Solubility product | Solubility product at 1200 °C |
|---------|---|----------------------------------|
| TiC | $\log[\text{Ti}][\text{C}] = -10475/T + 5.33$ | $[\text{Ti}][\text{C}] = 0.0165$ |
| VC | $\log[\text{V}][\text{C}] = -9500/T + 6.72$ | $[\text{V}][\text{C}] = 1.86$ |
| ZrC | $\log[\text{Zr}][\text{C}] = -8464/T + 4.26$ | $[\text{Zr}][\text{C}] = 0.0327$ |
| NbC | $\log[\text{Nb}][\text{C}] = -7900/T + 3.42$ | $[\text{Nb}][\text{C}] = 0.0114$ |
| TaC | $\log[\text{Ta}][\text{C}] = -7200/T + 2.90$ | $[\text{Ta}][\text{C}] = 0.0141$ |

where G , ε , r , and f are shear modulus, misfit strain, precipitate particle radius, and volume fraction of precipitated phase, respectively [8]. Misfit strain, ε , is proportional to difference in lattice constant between the precipitate phase and the matrix. The lattice constant of vanadium carbide differs from that of Fe–36%Ni austenite matrix about by 15%. Since other carbides, TiC, ZrC, NbC, and TaC, also have a form of NaCl structure but their lattice constants are too large for the carbides to precipitate coherently, the magnitude of precipitation strengthening could be largest for Invar-V.

Moreover, another reason for higher hardness of Invar-V might derive from denser and finer distribution of the carbides. When a dislocation moves with loops remained around particles, the necessary stress is estimated as follows:

$$\tau = Gb/l \quad (2)$$

where b and l are Burgers vector and the distance between particles, respectively [8]. Based on this Orowan bowing bypass model, the stress is inversely proportional to the spacing between precipitated particles. Since supersaturation of alloy carbide is much larger for Invar-V when aged at 650 °C, the number of precipitated particles is larger and thus they can be densely distributed. The combination of these mechanisms might be the reasons of superior hardening of Invar-V.

Thermal Expansion

Figure 4(a) shows dilation curves for Invar-Ti, V, Zr, and Nb as well as Fe–36 wt%Ni alloy in solution-treated condition. As is typical for Fe–36 wt%Ni alloy, thermal dilations were small near room temperature (“Invar region”) and became large rapidly beyond a temperature due to loss of the negative volume magnetostriction effect. Figure 4(b) summarizes the mean thermal expansion coefficients (TEC) in the temperature range from 50 to 150 °C, $\alpha_{50-150^\circ\text{C}}$. Regarding the effect of alloying elements, Ti and V gave rise to higher TEC than Zr and Nb in the Invar region as shown in Fig. 4(b). It is reported that TEC of

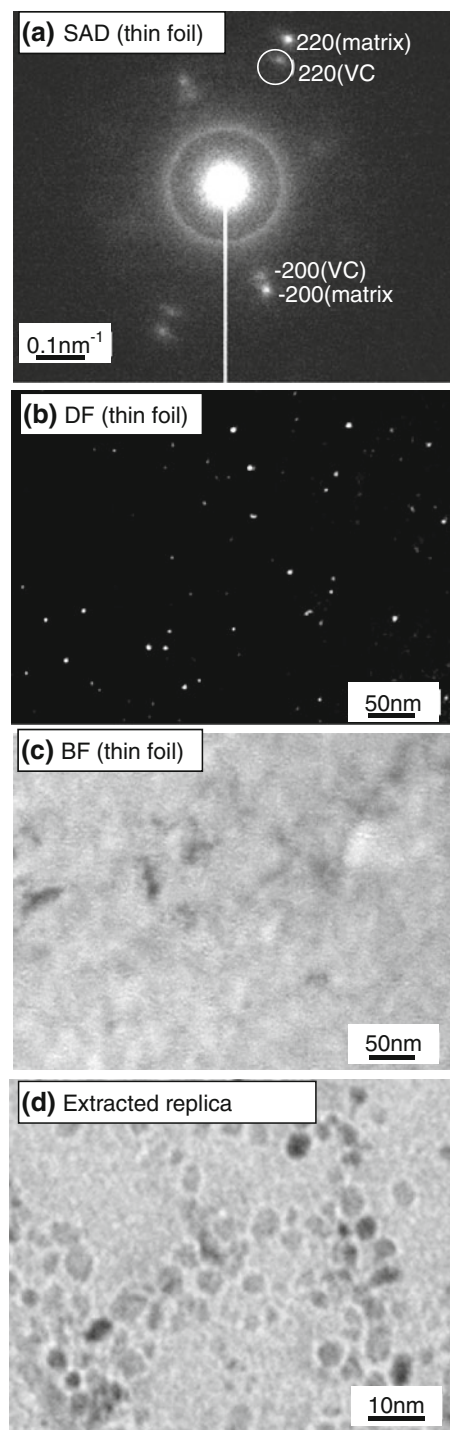


Fig. 3 Results of transmission electron microscope observation for Invar-V after aging at 650 °C: (a) a selected area diffraction pattern (SAD) obtained an area including VC and austenite matrix, (b) a dark-field image (DF) obtained from a diffracted beam circled in (a), (c) a bright-field image (BF) taken from the same area as (b), and (d) an image of extracted replica

Fe–36 wt%Ni in the temperature range from 30 to 100 °C increases with additions of other elements and the magnitudes of increment change element by element [9]. Among

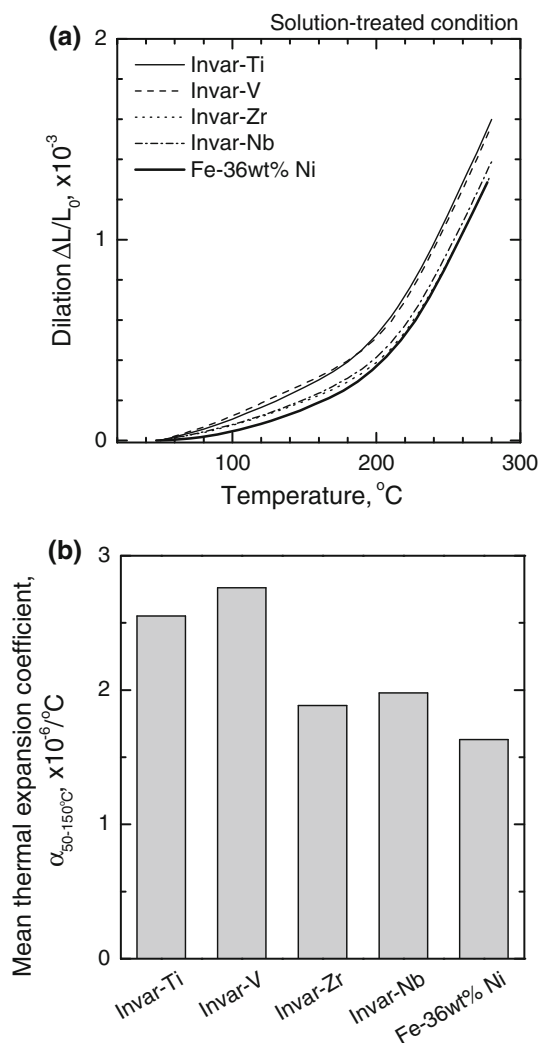


Fig. 4 Thermal expansion of Invar-X in solution-treated condition: (a) dilation curves and (b) mean thermal coefficients between 50 and 150 $^{\circ}\text{C}$

Ti, V, and Nb, it is reported that Ti has the largest influence on raising TEC and Nb the smallest. Although this result may appear inconsistent with the reported order, it is no wonder that Invar-V showed the highest TEC considering that the solubility product of $[X][C]$ at the solution treatment temperature was larger for Invar-V than for Invar-Ti and thus the amounts of V and C, which also raises TEC in solid solution, were much larger for Invar-V.

Conclusions

1. When the additives, Ti, V, Zr, Nb, and Ta, which form carbides in Fe–36 wt%Ni–0.2 wt%C alloy,

were compared in terms of age hardness, V had the strongest effect demonstrating the maximum hardness at aging temperature 650 $^{\circ}\text{C}$. On the other hand, Ti, Nb, and Ta showed weak secondary hardening while Zr did not show any secondary hardening.

2. In V-added Fe–36 wt%Ni–0.2 wt%C alloy, fine vanadium carbides with a size of 5 nm precipitated when aged at 650 $^{\circ}\text{C}$. Some of these carbides precipitated coherently with the matrix, which would enhance hardness by misfit strain as well as dense population of them. Other alloys with Ti, Zr, Nb, and Ta as additives contained more or less primary carbides.
3. Thermal expansion coefficients of V-added Fe–36 wt%Ni–0.2 wt%C alloy was the largest of the investigated alloys. This is mainly due to a large amount of dissolved V and C in the matrix. However, it would be expected that thermal expansion becomes small when V and C are eliminated from the matrix by aging.
4. For the purpose of developing a high-strength and low-thermal expansion alloy, the addition of V and C to Fe–36 wt%Ni alloy is one of preferable solution.

References

1. H. Saito, *Physics and applications of Invar alloys* (Maruzen, Tokyo, 1978)
2. M. Kishida, T. Masumoto, Applications of Invar-type alloys to various precision instruments. *Mater. Jpn.* **36**, 1080–1085 (1997). (in Japanese)
3. K. Suzuki, Application of Invar wire to overhead transmission line. *Mater. Jpn.* **36**, 1075–1079 (1997). (in Japanese)
4. S. Sasaki, T. Takebe, K. Miyazaki, M. Yokota, K. Sato, S. Yoshida, I. Matsubara, ZTACIR-new extra-heat resistant aluminum alloy conductor galvanized Invar reinforced. *Sumitomo Electr.* **125**, 54–60 (1984). (in Japanese)
5. K. Nakama, T. Kariya, T. Isomoto, M. Sanai, T. Nishikawa, Development of high strength invar alloy wire for ultra-high voltage power cable. *Mater. Jpn.* **49**, 69–71 (2010). (in Japanese)
6. K. Nakama, S. Furuya, K. Sugita, K. Inoue, Y. Shirai, Lattice defects of cold-drawn and aged Fe–36 wt%Ni alloys and effects of additions of C and V on hardness and thermal expansion. *Tetsu-to-Hagané* **99**, 380–389 (2013). (in Japanese)
7. K. Narita, Kochu no tankabutsu ni tsuite (II). *Bull. Jpn. Inst. Met.* **8**, 49–57 (1969). (in Japanese)
8. C.T. Sims, N.S. Stoloff, W.C. Hagel, *Superalloys II* (Wiley, New York, 1987), pp. 69–96
9. M. Tsuda, Effect of minor alloying elements on the mean thermal expansion coefficient of Fe–36%Ni Invar alloy. *Tetsu-to-Hagané* **80**, 944–949 (1994). (in Japanese)